Modulated Imaging in Layered Media

Jessie R. Weber, David J. Cuccia, Bruce J. Tromberg

***Abstract*— We present forward modeling and measurement of spatially modulated illumination in layered turbid tissue systems. This technique is used to provide quantitative, depth-resolved functional physiologic information with applications in layered tissues including cortex, retina and skin.**

I. Introduction

Many tissues, including the cortex of the brain, the retina and the skin, are composed of stratified, submillimeter layers. The human cortex is approximately 3mm thick with six layers which differ in cell size and type. The retina has seven layers (including a nerve fiber layer, choroid layer (blood supply), pigmented layer and photoreceptor layer) and ranges in total thickness from around 160 to 300um depending on location [1]. In the top layers of the skin, the epidermis thickness ranges from 0.5-1.5mm depending on location in the body, the dermis thickness ranges between 0.3-3mm and underneath the dermis is a thick layer of subcutaneous tissue. In rodent models, the skull is optically thin enough to for penetration of diffuse light, but its effects must be separated from those of the underlying neural tissues. In addition, many pathologies occur within a single layer, changing the size and/or physiologic functionality of that layer. If the optical properties of each layer could be resolved individually, we would have a powerful tool for diagnosis and tissue monitoring.

Modulated imaging (MI) uses broadband, spatially modulated light to provide maps of quantitative, functional physiologic information such as hemoglobin content, oxygen saturation and water content. It provides high temporal resolution and is noncontact and noninvasive and has depth sectioning capability. The instrument platform is shown in Figure 1 [2]. With these qualifications, MI is ideally suited for studying functional physiological changes in layered tissue. Currently, MI is capable of measuring the optical properties of a single layer, or single volume of tissue. The total depth of the volume sampled, δ, can be determined by the optical properties of the sample, μ_a (the absorption coefficient) and μ_s' (the reduced scattering coefficient), and the applied spatial frequency of the structured illumination, f_x. Different spatial frequencies probe different depths. The result is a map for quantitative optical properties within each *total* depth and a *qualitative* depth resolved image [2].

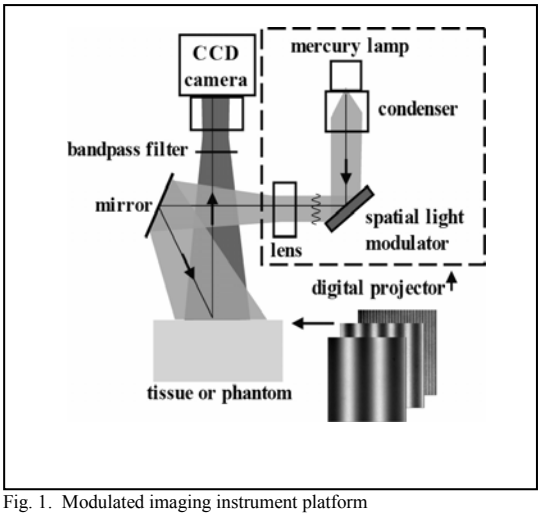

Fig. 1. Modulated imaging instrument platform

II. METHODS

We expanded an existing multilayer diffusion model of photon propagation [3] for use with spatially modulated incident light.

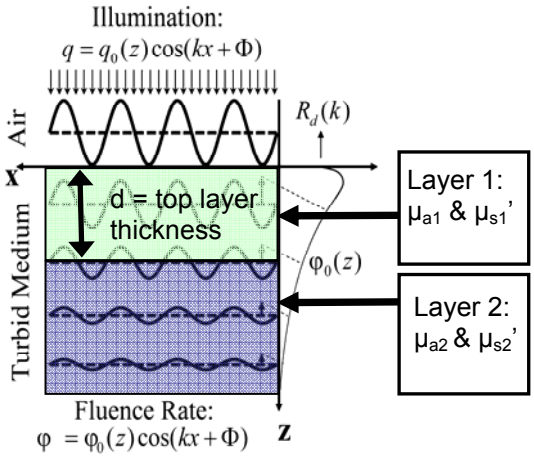

Fig.2. Cartoon of modulated illumination source and the resulting modulated internal fluence rate in a two layer model

In the two layer geometry shown in Figure 2, μa is the absorption coefficient, μs' is the reduced scattering coefficient, subscript 1 corresponds to the top layer, subscript 2 corresponds to the bottom layer, and d is the top layer thickness. These represent the five variables

Manuscript received April 28, 2006. This work was supported by the National Institutes of Health under grants P41-RR01192 (Laser Microbeam and Medical Program: LAMMP), the U.S. Air Force Office of Scientific Research, Medical Free-Electron Laser Program (F49620-00-2-0371 and FA9550-04-1-0101) and the Beckman Foundation.

All authors are with the Beckman Laser Institute and Medical Clinic, University of California, Irvine, Irvine, CA 92692.

J.R. Weber (phone: (949)824-8753, e-mail: weberjr@uci.edu).

D.J. Cuccia (e-mail: dcuccia@uci.edu).

B.J. Tromberg (e-mail: bjtrombe@uci.edu).

present in the model. The boundary conditions used for solving the diffusion equation are:

Fundamental

$$j \equiv \frac{1}{3\mu_{tr}} \frac{\partial \Phi}{\partial z}\bigg|_{z=0}$$

PartialCurrent

$$j = \frac{1 - R_{eff}}{2(1 + R_{eff})} \Phi \bigg|_{z=0}$$

$$\left(\Phi_1 = \Phi_2\right)\big|_{z=d}$$

$$\left(j_1 = j_2\right)\big|_{z=d}$$

where j is flux, Φ is the fluence rate, with subscripts 1 and 2 corresponding to the top and bottom layers, respectively, z is the axis normal to the surface of the sample, and R_{eff} is the effective reflection coefficient. Using the boundary conditions to solve for fluence in each layer and for flux at the surface,

$$\Phi_1 = S_1 e^{-\mu_{tr1} z} + A_1 e^{-\mu_{eff1}' z} + A_2 e^{+\mu_{eff1}' z}, 0 < z \le d$$

$$\Phi_2 = S_2 e^{-\mu_{tr2} z} + A_3 e^{-\mu_{eff2}' z}, z > d$$

$$\mu_{tr,i} = \mu_{s,i}' + \mu_{a,i}; \mu_{eff,i}' = \frac{1}{\partial_{eff,i}} = \sqrt{3\mu_{a,i}\mu_{tr,i} + (2\pi f_x)^2};$$

$$j\big|_{z=0} = -\eta R_d, \text{ where } \eta = \frac{1 - R_{eff}}{2(1 + R_{eff})}$$

R_d is diffuse reflectance, the value we measure with our CCD camera. δ_{eff} is the effective penetration depth, which is modified by the applied spatial frequency, f_x. At f_x=0, or planar/DC illumination, the equation reduces to the homogeneous form, only depending on the optical properties. Thus, using different spatial frequencies allows us to control the depth we are sampling.

Using this model, we designed and ran simulations in Matlab (The Mathworks, Inc.) for two layers with different optical properties (absorption and scattering), different top layer thicknesses and different modulation frequencies. These simulations allowed us to determine spatial frequency ranges would be ideally suited for resolving the optical properties in each layer. We then designed layer experiments using phantoms to verify the model.

III. RESULTS

A. Forward Modeling

Using the two layer model and varying each of the five parameters one at the time, we generated plots of Rd vs. spatial frequency. These plots, in Figure 3, show the amount of contrast in Rd for changes in optical properties (not considering noise).

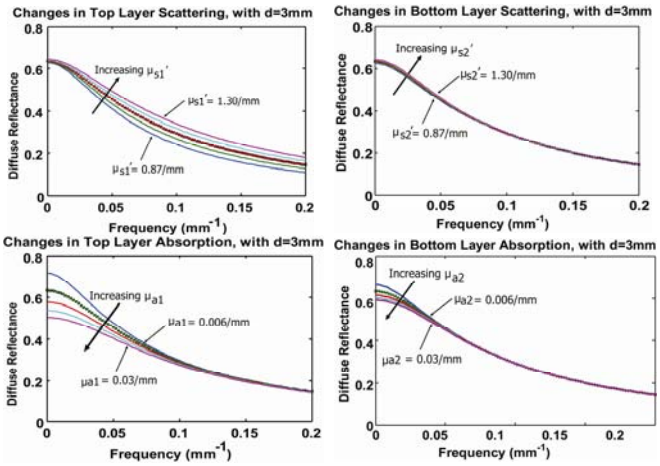

Fig. 3. Forward Plots: expected contrast in Rd vs. spatial frequency. Top: Changes in scattering, top and bottom layers on left and right, respectively. Bottom: Changes in absorption, top and bottom layers on left and right, respectively.

From these forward plots, we can see that low spatial frequencies are most sensitive to changes in absorption, while higher spatial frequencies contain scattering information. The low spatial frequencies probe more deeply than high spatial frequencies (according to the equation for δ_{eff}, in the derivation) which explains why bottom layer absorption has more predicted contrast than bottom layer scattering.

B. Measurements

We performed experiments to verify the two layer model. We began by varying either top layer scattering or absorption, keeping all other variables constant.

Liquid layer phantoms were constructed so that the optical properties in the top layer could be varied. Intralipid (soybean oil) was used as a scatterer and water soluble nigrosin as an absorber. The liquid layers were separated by an thin layer of mylar material, and the bottom layer was deep enough to be considered semi-infinite (several cm). The parameters chosen for the liquid phantoms appear below in Table 1.

The phantoms were measured at 660nm with 42 spatial frequencies from 0-0.2/mm. The measured and predicted results appear below in Figure 4.

TABLE I

Phantom Parameters	Variable	Constant Value	Varied Value (when varied)
Top layer thickness	d	3mm	Not varied
Absorption Coefficient	μa	0.011/mm	0.006 – 0.03/mm
Scattering Coefficient	μs'	1.1/mm	0.9 – 1.3/mm

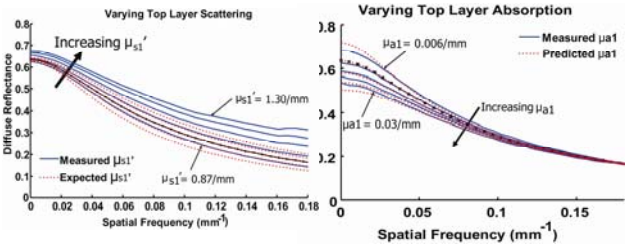

Fig. 4. Measured and expected Rd vs. spatial frequency.

Using these results and fitting to the two layer model with different combinations and numbers of variables, we were able to reconstruct the values for top layer absorption and for top layer scattering as shown in Figure 5.

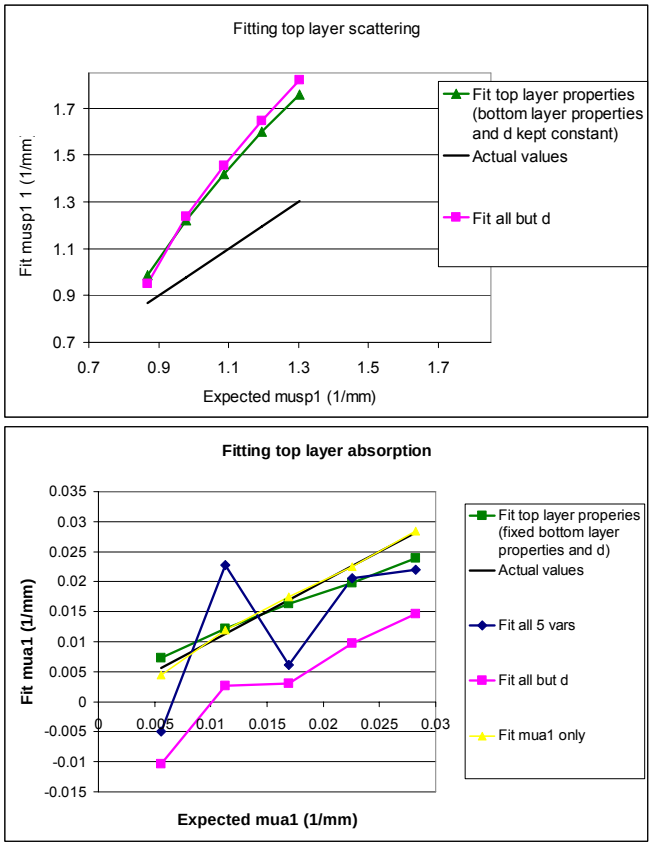

Fig. 5. Top: 4-variable and 2-variable fits for top layer scattering. Bottom: 5-variable, 4-variable, 2-variable and 1-variable fits for top layer absorption.

IV. Conclusion

We report preliminary progress of spatial frequency domain modeling and measurement of layered structures. The results presented here indicate correspondence between predicted and measured diffuse reflectance values versus spatial frequency for changes in top layer optical properties. Correct trends were recovered for optical property values from changes in the top layer.

References

[1] M. Shahidi, W. Zhangwie, and R. Zelkha. "Quantitative Thickness Measurement of Retinal Layers Imaged by Optical Coherence Tomography," Am J Ophthalmol. 2005 Jun;139(6):1056-61.

[2] D.J. Cuccia, F. Bevilacqua, A.J. Durkin, and B.J. Tromberg. "Modulated imaging: quantitative analysis and tomography of turbid media in the spatial-frequency domain," Opt Lett. 2005 Jun 1;30(11):1354-6..

[3] L.O. Svaasand, T. Spott, J.B. Fishkin, T. Pham, B.J. Tromberg and M.W. Berns. "Reflectance measurements of layered media with diffuse photon-density waves: a potential tool for evaluating deep burns and subcutaneous lesions," Phys. Med. Biol. 44(1999) 801-813.

[4] B. Smith, "An approach to graphs of linear forms (Unpublished work style)," unpublished.

[5] E. H. Miller, "A note on reflector arrays (Periodical style—Accepted for publication)," *IEEE Trans. Antennas Propagat.*, to be published.

[6] J. Wang, "Fundamentals of erbium-doped fiber amplifiers arrays (Periodical style—Submitted for publication)," *IEEE J. Quantum Electron.*, submitted for publication.

[7] C. J. Kaufman, Rocky Mountain Research Lab., Boulder, CO, private communication, May 1995.

[8] Y. Yorozu, M. Hirano, K. Oka, and Y. Tagawa, "Electron spectroscopy studies on magneto-optical media and plastic substrate interfaces(Translation Journals style)," *IEEE Transl. J. Magn.Jpn.*, vol. 2, Aug. 1987, pp. 740–741 [*Dig. 9th Annu. Conf. Magnetics* Japan, 1982, p. 301].

[9] M. Young, *The Techincal Writers Handbook.* Mill Valley, CA: University Science, 1989.

[10] J. U. Duncombe, "Infrared navigation—Part I: An assessment of feasibility (Periodical style)," *IEEE Trans. Electron Devices*, vol. ED-11, pp. 34–39, Jan. 1959.

[11] S. Chen, B. Mulgrew, and P. M. Grant, "A clustering technique for digital communications channel equalization using radial basis function networks," *IEEE Trans. Neural Networks*, vol. 4, pp. 570–578, July 1993.

[12] R. W. Lucky, "Automatic equalization for digital communication," *Bell Syst. Tech. J.*, vol. 44, no. 4, pp. 547–588, Apr. 1965.

[13] S. P. Bingulac, "On the compatibility of adaptive controllers (Published Conference Proceedings style)," in *Proc. 4th Annu. Allerton Conf. Circuits and Systems Theory*, New York, 1994, pp. 8–16.

[14] G. R. Faulhaber, "Design of service systems with priority reservation," in *Conf. Rec. 1995 IEEE Int. Conf. Communications*, pp. 3–8.